

Automatic 3D Mesh Generation of Multiple Domains for Topology Optimization Methods

Jean-Christophe Cuillière¹, Vincent Francois¹, Jean-Marc Drouet²

¹ÉRICCA, Université du Québec à Trois-Rivières, Québec, Canada, jean-christophe.cuilliere@uqtr.ca, vincent.francois@uqtr.ca.

²Groupe Optis, Université de Sherbrooke, Québec, Canada, jean-marc.drouet@usherbrooke.ca.

Abstract – This paper presents an automatic approach to generate unstructured tetrahedral meshes in the context of composite or heterogeneous geometry. Using B-Rep concepts and specific adaptations of advancing front mesh generation algorithms, this approach guarantees, in a simple and natural way, mesh continuity and conformity across the interior boundaries of a composite domain. This method presents a great potential in various fields of application such as finite element simulations (in the case of heterogeneous materials and assemblies for example), animation and visualization (medical imaging for example). After a description of the approach and its context, the paper presents a potential application in the specific domain of topology optimization.

Keywords: Mesh generation, multiple domains, B-Rep, CAD/FEA integration, topology optimization.

1. Introduction

With numerical methods in general, among which finite element analysis (FEA), being used in many different fields of activity and in many different types of applications, there is an emerging need for the adaptation of automatic mesh generation procedures to a great number of very different contexts. Medical imaging, multi-physics or multi-phases simulations, multiple parts and multi-materials simulations in engineering design are several examples of these specific contexts. In general there is an increasing need for automatically generating high quality FEA meshes over various types of domains with respect to various types of constraints. Automatically generating FEA meshes over multiple domains, while satisfying size, quality and continuity requirements is an example of these specific constraints, which is likely to be used for many applications such as visu-

alization, numerical simulations or imaging for example [1-4]. This paper focuses on the development of a specific adaptation of the advancing front mesh generation method (AFM) aimed at the automatic generation of well sized and shaped tetrahedrons over multiple domains. This adaptation has many potential applications, among which its use in the context of integrating topology optimization methods with computer aided design (CAD) as illustrated in this paper.

The paper starts with the problem statement (generating a valid and continuous 3D mesh over 3D heterogeneous geometry) in the next section. After this, section 3 focuses on the way this heterogeneous geometry is modeled using specific boundary representation (B-Rep) concepts while section 4 is dedicated to the presentation of the automatic mesh generation scheme proposed. Section 5 presents results obtained in the context of topology optimization and section 6 draws conclusions and outlines future work.

2. Problem statement

For various reasons and for many applications, there is a need for being able to describe a given closed domain Ω of the 3D space with a heterogeneous representation of geometry. It is the case for example when Ω is physically composed of an assembly of heterogeneous materials for which a specific sub-domain must be defined for each type of material. Generally speaking, given a heterogeneous and closed geometric domain Ω , it can be divided into $N+1$ closed regions or sub-domains Ω_i so that the union of all $\bigcup_{i=0}^N \Omega_i$ equals Ω . A common problem consists of automatically generating $N+1$ meshes of the regions or sub-domains Ω_i and tagging each elements as belonging to one of the Ω_i , while globally obtaining a continuous and conformal mesh of Ω when these $N+1$ meshes are put together. Once the problem stated this way, one of the most sensitive issues in adapting standard mesh generation procedures, either Delaunay, advancing front or octree based [5] to this specific context is how sub-domains Ω_i are defined. As introduced in the next section, sub-domains Ω_i can be defined in many different ways, which has a major impact on how standard mesh generation procedures can be adapted, and how mesh conformity and continuity can be insured at the interface between the sub-domains in contact. In the work presented here, the specific objective is developing a mesh generation tool for integrating topology optimization into the CAD process.

3. Heterogeneous geometry

3.1 General considerations

Given a closed 3D domain Ω (with B defined as the boundary of Ω) divided into $N+1$ sub-domains Ω_i (with B_i defined as the boundary of Ω_i). The sub-domains Ω_i themselves and/or the frontiers (a subset of $\bigcup_{i=0}^N B_i$) between these sub-domains can be defined either explicitly (sets of B-Rep models for example) or implicitly (with respect to the definition of a background cartesian grid of octree structure where cells are classified with respect to the sub-domains Ω_i). Also, the frontiers between sub-domains can be defined either exactly (as an analytically defined free-form surface for example as it is the case in the work presented here) or approximately (as a triangulation like in [1-2]). For example, a common and quite easy way (see [4]) used to define multiple sub-domains Ω_i is introducing a specific octree structure in which each cell is classified with respect to its belonging to the interior or boundary of some of the sub-domains Ω_i . In this case, the boundaries B_i and, by the way, the frontiers between two or more sub-domains Ω_i are defined implicitly through the definition, on the edges of cells, of intersection points (in the case of primal contouring or marching cubes methods) and of normal vectors (in the case of dual contouring methods). Such an implicit definition of frontiers is usually referred to as isocontouring [4]. Another issue, which as a major impact on which mesh generation approach is likely to be used is that in some cases, the union of boundaries $\bigcup_{i=0}^N B_i$ can be either manifold or non-manifold like illustrated (on a 2D case for more clarity) in Figure 1.

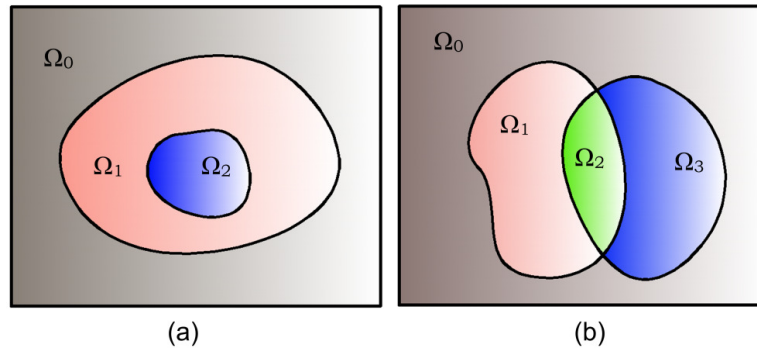


Fig. 1. Sub-domains with (a) a manifold boundary topology and (b) a non-manifold boundary topology.

3.2 Topology optimization

The design optimization of any type of component is based on iteratively applying several finite element analyses (FEA) to induce gradual shape and topology enhancements. Several methods have been introduced aimed at the automation of this optimization process, among which topology optimization methods [6-10]. The great potential of these approaches is that the shape and topology evolution is not constrained by the initial topology and this leads to results where the final topology is not known a priori. By the way, both shape and topology are optimized which is likely to be very powerful in the context of product development with computer aided design (CAD). Input data required by these methods typically stands as an initial 3D geometry along with the specification of subsets of this initial geometry that should not be affected by the optimization process. For example, material around fastening holes or, more generally, material around geometric features on which boundary conditions are applied should not be modified by the optimization. All subsets of the initial geometry that must be kept intact are referred to as the *non-design sub-domain*. The remainder of the initial geometry is composed with material which is likely to be remodeled. This latter subset of the initial geometry is referred to as the *design sub-domain*. Most topology optimization methods require that *non-design* and *design* geometries must be meshed so that finite elements are tagged as *design* and *non-design* elements and so that continuity and conformity is guaranteed at the interface between *design* and *non-design* sub-domains. These mesh generation requirements inherent to topology optimization methods are part of the general context presented above with Ω corresponding to the entire geometry, $\bar{\Omega} = \bigcup_{i=1}^N \Omega_i$ corresponding to the *non-design* sub-domain (composed with N disconnected volumes Ω_i) and $\Omega_0 = \Omega - \bar{\Omega}$ to the *design* sub-domain.

3.3 B-Rep definitions of Ω and $\bar{\Omega}$.

In this work, the definition of Ω and its sub-domains Ω_i is made using boundary representation (B-Rep) concepts. A first B-Rep is defined for Ω and a second B-Rep for $\bar{\Omega} = \bigcup_{i=1}^N \Omega_i$. Thus, the *design* sub-domain Ω_0 is not defined explicitly. An interesting aspect of the method is that it does not require, as input, any definition or triangulation of interior boundaries at the interface between the Ω_i . The triangulation of these boundaries will be generated through the mesh generation process itself. Figure 2 illustrates, on a sample part, these two B-Rep models: one associated with Ω (Figure 2b) and the other associated with $\bar{\Omega} = \bigcup_{i=1}^3 \Omega_i$ (Figure 2c).

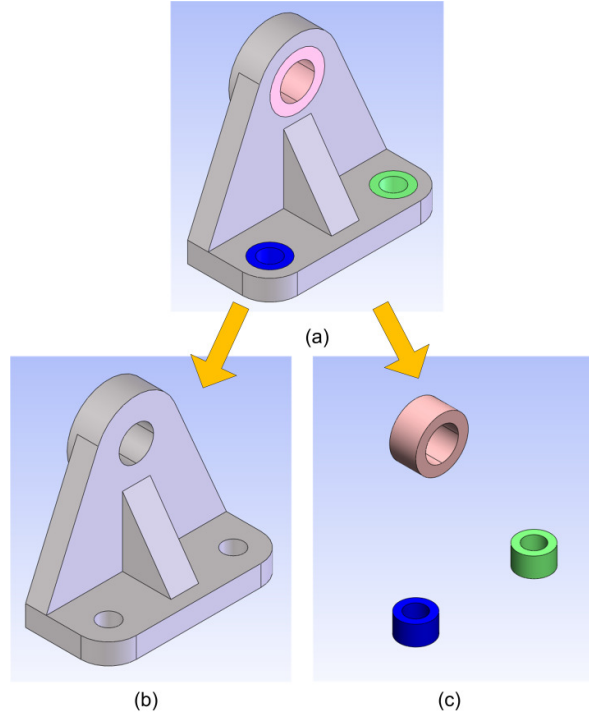


Fig. 2. The B-Rep definition of Ω and $\bar{\Omega} = \cup_{i=1}^3 \Omega_i$.

B-Rep structures [11-12] have been used for many years in the context of 3D modelling and are very classical data structures aiming at a concise representation of 3D solid topology (vertices, edges, faces, volumes, etc.) and underlying geometry (points, curves and surfaces). One of the interests of using B-Rep structures as a basis for mesh generation is that its hierarchical structure is very appropriate for integrating it with the hierarchical structure of mesh components as illustrated in Figure 3. In fact, this integration is classically related to the mesh generation process itself as the automatic discretization of a 3D solid object is usually performed following steps that are consistent with the B-Rep topological hierarchy (generating nodes on B-Rep vertices, mesh segments along B-Rep edges, mesh triangles on B-Rep faces and finally mesh tetrahedrons inside the B-Rep volume). This *close integration between B-Rep topology and mesh components is the cornerstone of the mesh generation process* presented in the following section.

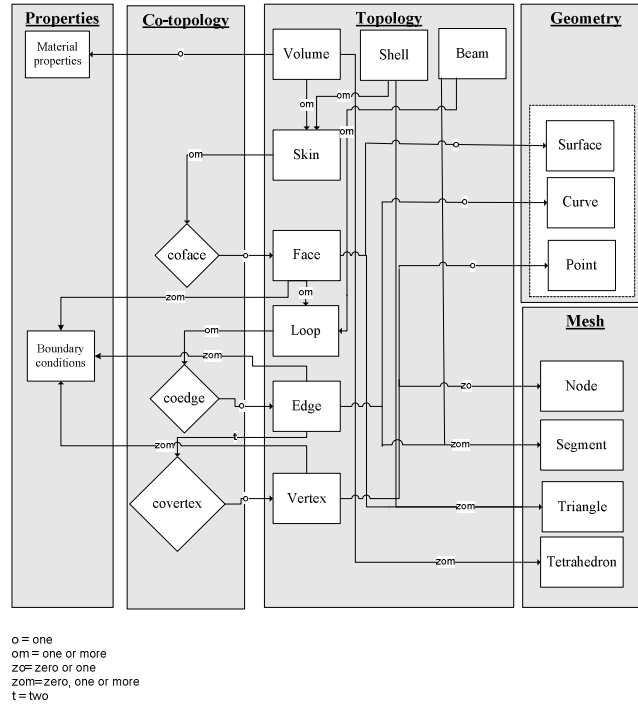


Fig. 3. The B-Rep data structure and its integration with FEA data.

4. Meshing heterogeneous geometry

4.1 Introduction

In the work presented here, automatically meshing multiple sub-domains in contact is performed by an adaptation of existing mesh generation procedures developed by our research team [13-15], which is based on a specific and new adaptation of the AFM. As mentioned in the previous paragraph, Ω and $\bar{\Omega} = \bigcup_{i=1}^N \Omega_i$ are defined using two separate B-Rep models. This specific definition of geometry implies using specific mesh generation procedures. Both Ω and $\bar{\Omega} = \bigcup_{i=1}^N \Omega_i$ must be meshed so that each finite element generated can be tagged as located inside one of the sub-domains Ω_0 to Ω_N and so that *continuity and conformity of the mesh can be guaranteed* across each frontier between any sub-domains in contact.

In the case of standard mesh generation processes, discretizing any type of B-Rep entity (a vertex, an edge, a face or a volume) is performed from scratch, which means that no nodes and elements have already been partially generated on these entities. In this work, the adaptation of standard mesh generation procedures to meshing multiple sub-domains in contact basically relies on adapting these procedures to partially meshed entities (vertices, edges, faces and volumes) such as meshing the remainder of a volume that is already partially filled with tetrahedrons. This is due to the fact that it is necessary to make sure that the mesh of each sub-domain is performed with *respect to constraints imposed by the mesh of other sub-domains in contact* and vice versa. This adaptation follows the same general steps as for standard mesh generation procedures, which means consistently with the B-Rep topological hierarchy. Thus, the process starts with generating nodes on some of the B-Rep vertices, which is followed by partially meshing edges, faces and volumes. Partially meshing B-Rep vertices and edges is quite straightforward and will not be described here.

4.2 Partially meshing B-Rep faces and volume

Partially meshing a B-Rep face or a B-Rep volume is basically performed with the AFM through specific adaptations of the advancing front initiation. These adaptations are first illustrated for partially meshed B-Rep faces on a very simple case introduced in Figure 4 (a rectangular prism which is partially filled with tetrahedrons). In Figure 4, a colour convention has been used for more clarity: boundary triangles (lying on B-Rep faces) are red whereas internal triangles are light blue.

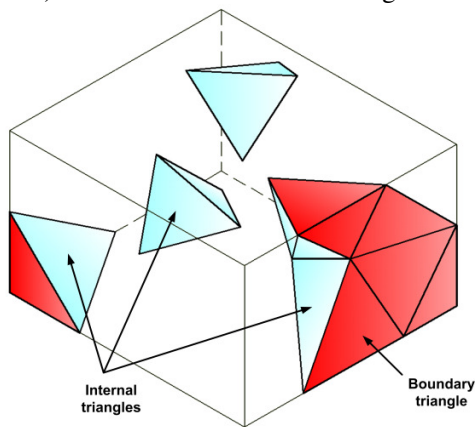


Fig. 4. A rectangular prism partially filled with tetrahedrons.

From this point, the complete triangulation of partially triangulated B-Rep faces is performed using the AFM combined with a specific initiation of the advancing front as illustrated in Figure 5 for a first B-Rep face. Figure 6 illustrates two specific cases occurring when existing isolated tetrahedrons connect inside B-Rep faces through isolated segments or isolated nodes.

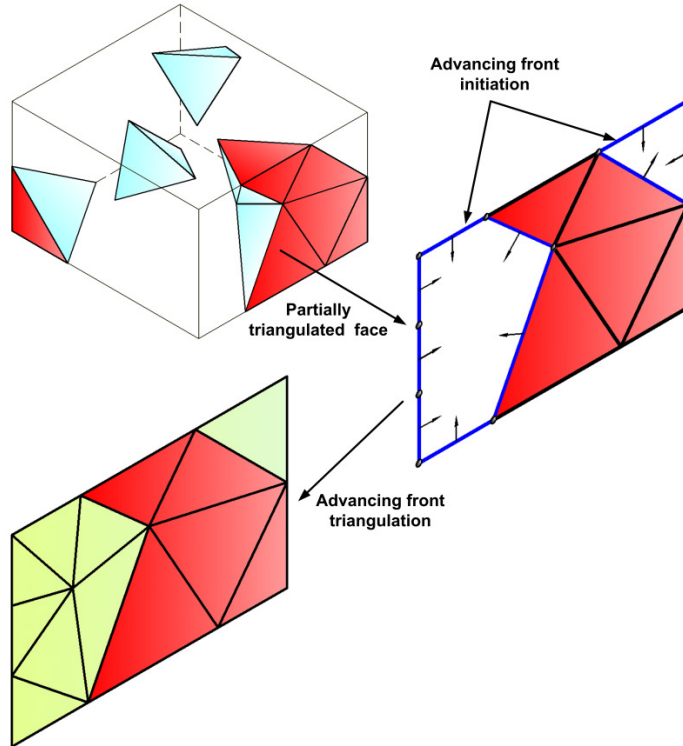


Fig. 5. Specific initiation of the AFM for partially triangulated B-Rep faces.

These situations (isolated segments and isolated nodes) require further processing. In the case of an isolated segment, the advancing front is initiated on this segment using a pair of front elements (segments) which are oriented in opposite directions. For an isolated node, a first option is creating an arbitrary pair of mesh segments issued from the isolated node. This ensures that the resulting mesh will feature the isolated node. However, if many isolated nodes have to be processed on a given B-Rep face, this option is likely to fail because it will be difficult if impossible to generate many arbitrary pairs of mesh segments without interference. Alternate options for taking into account isolated nodes are constrained meshing or *a*

posteriori mesh adaptation. It is important to point out that specific configurations may occur when processing isolated segments, for example when an isolated segment connects with the face's boundary. An elegant and efficient way to handle these specific configurations is using a non-manifold data structure for the advancing front, in which (in 2D) a front node can be shared by more than two front segments.

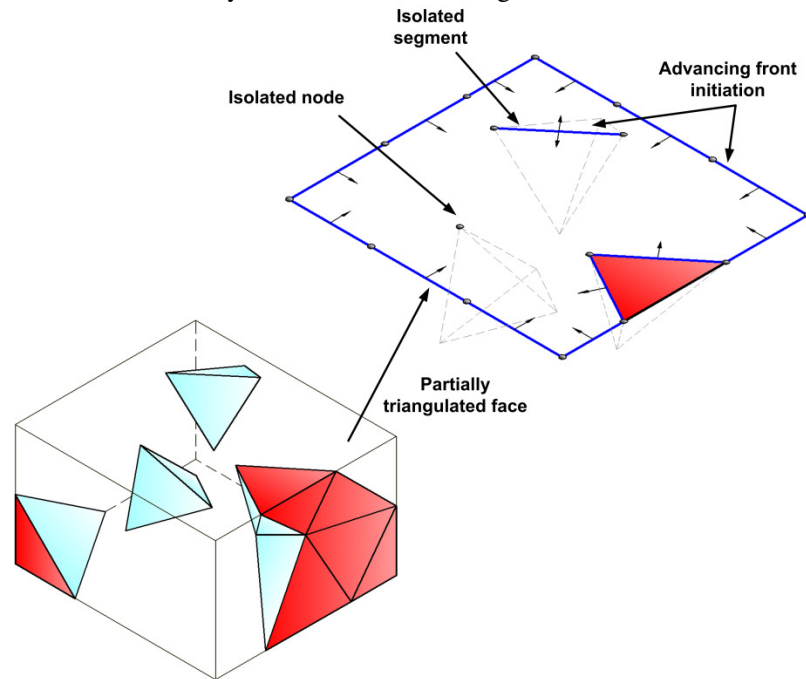


Fig. 6. Initiation of the AFM for partially triangulated B-Rep faces with an isolated segment and an isolated node.

Once each B-Rep face is processed this way, the AFM can be initialized for the automatic generation of tetrahedrons inside the remaining volume to be filled. Here again, this initialization needs to be adapted to the context. The 3D advancing front (composed with sets of triangles) is basically initialized with all triangles generated at the previous step along with all triangular faces of existing tetrahedrons that are located inside the B-Rep volume. Moreover, specific configurations have to be handled through further processing, like in the case of the partial triangulation of B-Rep faces. These specific configurations may occur, in a general context, with the presence of isolated mesh nodes, segments and faces inside the B-Rep volume. These specific configurations are dealt with using the same basic

principles as those described in the case of the partial triangulation of B-Rep faces for isolated nodes and segments. This involves handling a non-manifold data structure for the 3D advancing front, which practically cannot be avoided for the 3D implementation of the advancing front method in general. Being able to handle partially meshed B-Rep vertices, edges, faces and volumes, along with maintaining a close integration between B-Rep topology and mesh components throughout the whole process are fundamental pre-requisites for the new mesh generation process presented in the next section.

4.3 A mesh generation process in 14 steps

The new mesh generation process presented in this paper is divided into 14 basic steps, which are necessary to make sure that the mesh of each sub-domain is performed with respect to constraints imposed by the mesh of other sub-domains in contact. We introduce this 14 steps process on the example illustrated in Figure 7 (bike suspension rocker).

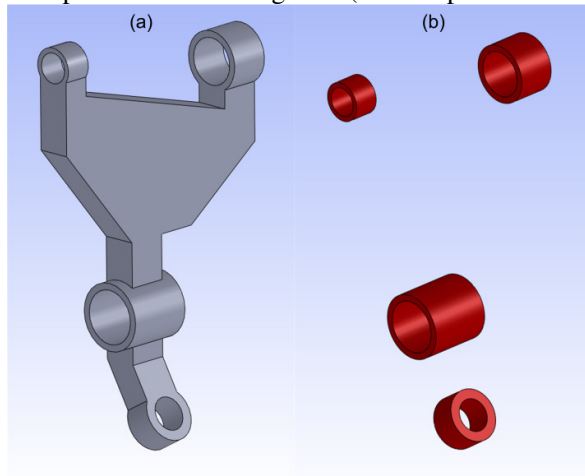


Fig. 7. a) Bike suspension rocker Ω b) The *non-design* sub-domain $\bar{\Omega} = \cup_{i=1}^4 \Omega_i$.

Basically, the mesh generation process follows the B-Rep structure's hierarchy and, at each stage of this hierarchy, the fundamental principle underlying these 14 steps is transferring mesh elements (nodes, straight lines, triangles and tetrahedrons) from one B-Rep model to the other one and so on. At the end, this back and forth process between the two models insures conformity and continuity of the resulting mesh. At each step of this back and forth process between the two models, the close integration between

B-Rep topology and mesh components allows enforcing a conforming mesh between sub-domains in contact without imprinting the geometries. In general, this basic framework can be applied in any situation where the generation of a given mesh is constrained by continuity and conformity conditions induced from an existing mesh or existing mesh elements.

Step 1: Generate nodes on the vertices of Ω (Figure 8).

Step 2: Transfer the nodes generated at step 1 that are also on vertices of $\bar{\Omega}$ to these vertices in $\bar{\Omega}$.

Step 3: Generate nodes on the remaining vertices of $\bar{\Omega}$ (Figure 9).

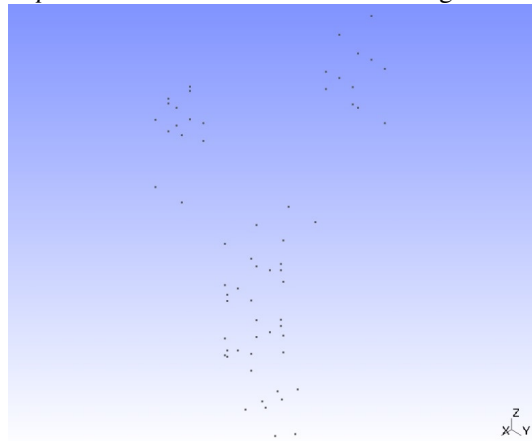


Fig. 8. Meshing the vertices of Ω .

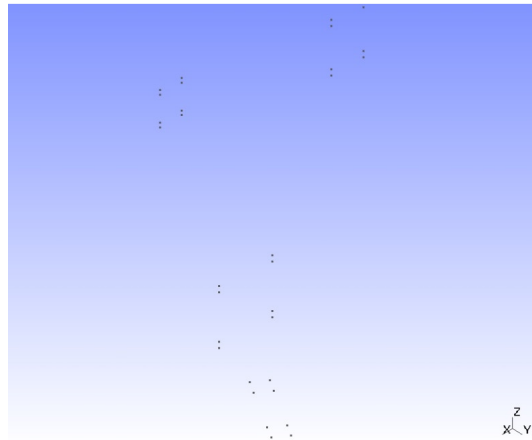


Fig. 9. Partially meshing the vertices of $\bar{\Omega}$.

Step 4: Transfer the nodes generated at step 3 that are located on edges of Ω to these edges in Ω .

Step 5: Mesh all the edges of Ω (with line segments) while taking into account the nodes that are already located along some edges after applying step 4. These nodes will later constrain the resulting mesh (Figure 10).

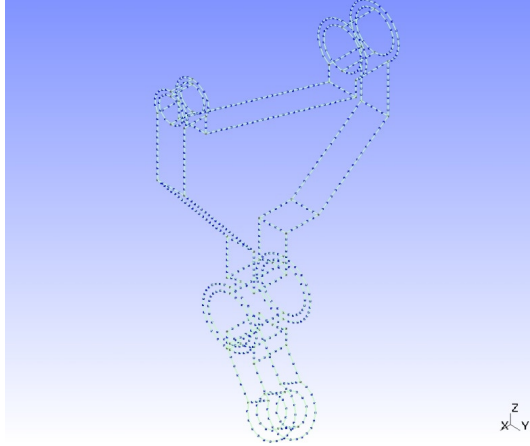


Fig. 10. Meshing B-Rep edges of Ω .

Step 6: Transfer the mesh segments generated at step 5 that are lying on edges of $\bar{\Omega}$ to these edges in $\bar{\Omega}$.

Step 7: Use a partial meshing algorithm to complete the mesh of all edges of $\bar{\Omega}$ (Figure 11).

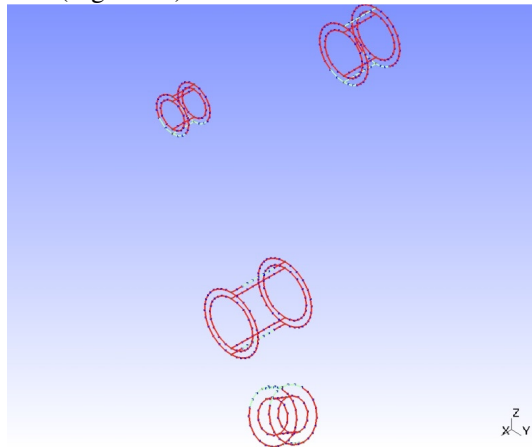


Fig. 11. Meshing the B-Rep edges of $\bar{\Omega}$. Mesh segments created at step 6 are in red while mesh segments created at step 7 are in green.

Step 8: Transfer the mesh segments generated at step 7 that are lying on faces of Ω to these faces in Ω .

Step 9: Triangulate all the faces of Ω taking into account edges that are already lying on some faces of Ω after applying step 7 (Figure 12).

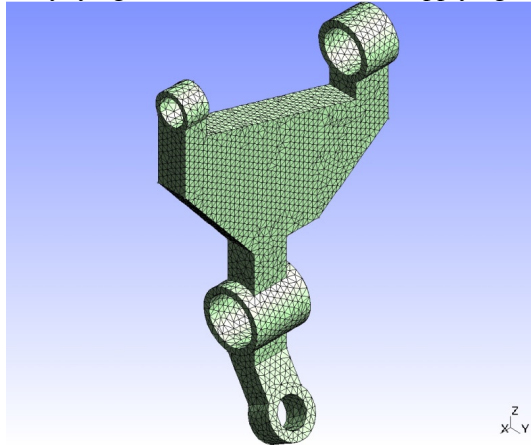


Fig. 12. Meshing all B-Rep faces of Ω .

Step 10: Transfer the mesh triangles generated at step 9 that are lying on faces of $\bar{\Omega}$ to these faces in $\bar{\Omega}$ (coloured red in Figure 13).

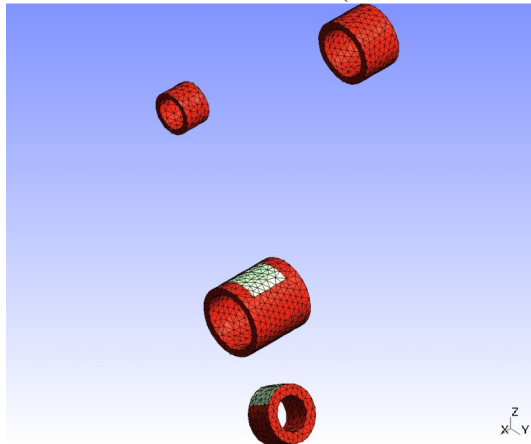


Fig. 13. Meshing all B-Rep faces of $\bar{\Omega}$. Mesh triangles created at step 10 are in red while mesh triangles created at step 11 are in green.

Step 11: Triangulate all the faces of $\bar{\Omega}$ while taking into account the triangles that are already lying on some faces after applying step 10. The new triangles generated at this step are coloured green in Figure 13.

Step 12: This step consists of filling the volume of $\bar{\Omega}$ with tetrahedrons using the standard AFM in 3D (Figure 14).

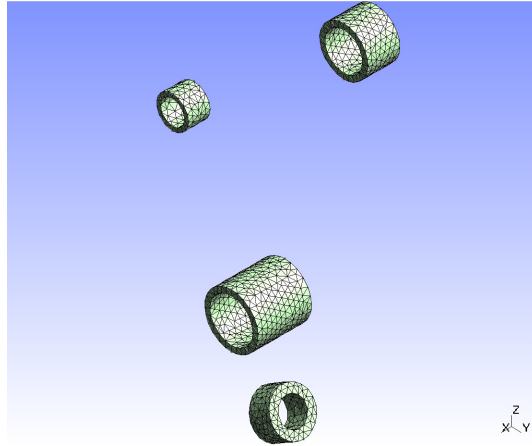


Fig. 14. Meshing the volume of $\bar{\Omega}$.

Step 13: Transfer the mesh tetrahedrons generated at step 12 to Ω

Step 14: Fill the remainder of Ω with tetrahedrons while taking into account the tetrahedrons (coloured red in Figure 15) transferred at step 13.

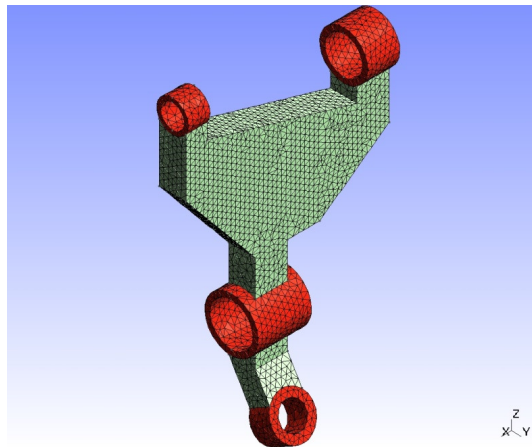


Fig. 15. The final mesh.

Once applied this 14 steps process, finite elements are tagged as part of Ω_0 (coloured green in Figure 15) or part of one of the Ω_i among $\bar{\Omega} = \bigcup_{i=1}^N \Omega_i$ (coloured red in Figure 15) and the continuity of the mesh at the interface between *design* and *non-design* sub-domains is guaranteed. It is worth mentioning that this approach can easily be combined with virtual topology concepts [14, 16], which means that either actual or virtual topology of the B-Rep can be considered when applying this 14 steps mesh generation process.

5. Application to topology optimization

The mesh generation process described in the previous section has been successfully implemented and integrated inside a topology optimization platform based on C++ code and on Code_AsterTM as a FEA solver. The optimization method used is an adaptation (to 3D unstructured meshes) of a solid isotropic material with penalization (SIMP) scheme. This choice is arbitrary as any other 3D topology optimization scheme that handles unstructured tetrahedral meshes could also have been used here. We used GmshTM [17] for visualizing SIMP results and the process is fully automated, starting from the input of the two B-Rep models introduced in section 3 (one for Ω and one for $\bar{\Omega}$) and a set of SIMP parameters. The basic principle on which the SIMP method is based is to consider the *design* domain $\Omega_0 = \Omega - \bar{\Omega}$ as a sort of “porous” material associated with a relative density distribution $\rho(x, y, z)$ ($\rho = 0$ represents void and $\rho = 1$ “full” or actual material). The field $\rho(x, y, z)$ is updated across the *design* domain through several FEA iterations until convergence on the part’s or structure’s compliance (see reference [7] for the detailed description of the SIMP method). At the beginning of the optimization process the relative distribution is initiated as a constant field $\rho(x, y, z) = f$ across Ω_0 . The constant f is defined as the volume fraction and represents the main constraint on the SIMP process, which basically expresses the fraction of *design* material which has to be retained from the initial *design* geometry throughout the process. For example, once the bike suspension rocker introduced in Figure 7 is meshed using the process presented in the previous section (see Figure 15) and once applied boundary conditions as illustrated in Figure 16a, applying the SIMP method (with $f = 0.2$) leads to a relative density distribution $\rho(x, y, z)$ shown in Figure 16b (without filtering) and Figure 16c (filtered using a Gaussian filter). This relative density distribution can then be derived into a 3D shape using a threshold on $\rho(x, y, z)$ as illustrated in Figures 17a and 17b. To obtain a more regular boundary and

by the way a more regular shape, the boundary triangulation of the *design* domain induced from the 3D mesh shown in Figure 17b can be smoothed (see Figure 17c) using various algorithms such as those described in [18].

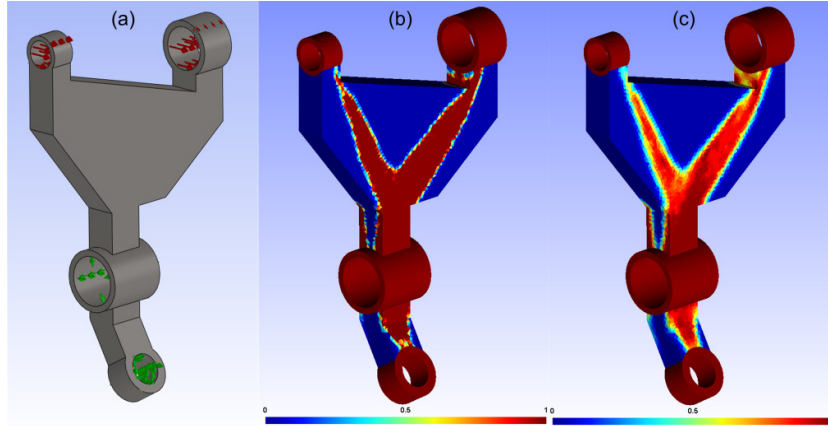


Fig. 16. a) Boundary conditions Ω b) Non filtered final $\rho(x, y, z)$ c) $\rho(x, y, z)$ after applying a Gaussian filter.

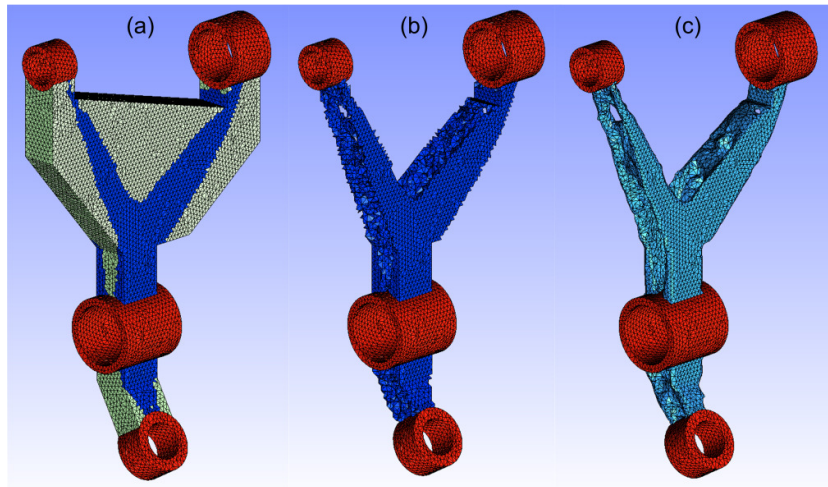


Fig. 17. Final shape obtained after applying a threshold on $\rho(x, y, z)$ for the result illustrated in Figure 16b, without smoothing the boundary triangulation (b) and after smoothing the boundary triangulation (c).

An interesting alternative consists of applying a Gaussian filter at each step of the SIMP process, which leads to more regular results as illustrated in Figure 18 for the same sample part with the same boundary conditions.

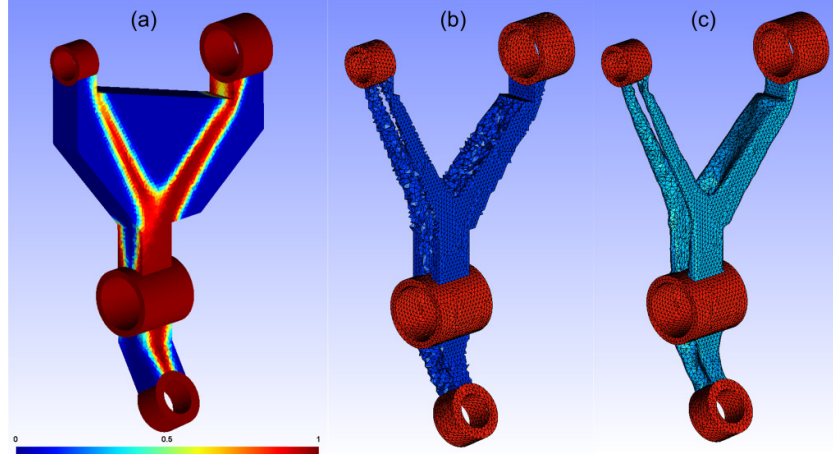


Fig. 18. Raw result and final shape obtained (before and after smoothing the boundary triangulation) in the case of applying a Gaussian filter on $\rho(x, y, z)$ at each iteration along the SIMP process.

6. Conclusion and perspectives

The new mesh generation tool presented in this paper has initially been designed for the automatic meshing of *design* and *non-design* sub-domains in the context of topology optimization methods but it is likely to be successfully applied in the more general context of meshing heterogeneous geometry. By using a back and forth process between B-Rep models associated with sub-domains Ω_i underlying heterogeneous geometry, along with a close integration between B-Rep topology and mesh components, a conforming mesh between sub-domains in contact can be obtained without imprinting the geometries and without requiring, as input, the definition or triangulation of boundaries at the interface between the Ω_i . At this point, the major issue in extending this method to heterogeneous geometry in general is that its implementation has been made in a specific context where each of the Ω_i in $\bar{\Omega} = \bigcup_{i=1}^N \Omega_i$ is in contact with Ω_0 only (which is always the case in the context of topology optimization). In the case of mutual contacts between the Ω_i in $\bar{\Omega} = \bigcup_{i=1}^N \Omega_i$ the method requires a significant adaptation, which is part of our current research interest.

References

1. Juretic, F., *Conformal Meshing of Multiple Domains in Contact*, in *International Meshing Roundtable*. 2008: Pittsburgh.
2. Sullivan Jr, J.M., G. Charron, and K.D. Paulsen, *A three-dimensional mesh generator for arbitrary multiple material domains*. *Finite Elements in Analysis and Design*, 1997. 25(3-4): p. 219-241.
3. Togashi, F., et al., *Extensions of overset unstructured grids to multiple bodies in contact*. *Journal of Aircraft*, 2006. 43(1): p. 52-57.
4. Zhang, Y., T.J.R. Hughes, and C.L. Bajaj, *An automatic 3D mesh generation method for domains with multiple materials*. *Computer Methods in Applied Mechanics and Engineering*, 2010. 199(5-8): p. 405-415.
5. Frey, P.J. and P.-L. George, *Mesh generation : Application to finite elements*, ed. Wiley. 2008.
6. Beckers, M., *Topology optimization using a dual method with discrete variables*. *Structural Optimization*, 1999. 17: p. 14-24.
7. Bendsoe, M.P. and O. Sigmund, *Topology optimization - Theory, Methods and Applications*. 2nd ed. 2003, Berlin: Springer. 370.
8. Bruns, T.E., *A reevaluation of the SIMP method with filtering and an alternative formulation for solid-void topology optimization*. *Struct. Multidisc. Optim.*, 2005. 30: p. 428-436.
9. Sigmund, O., *Topology optimization : a tool for the tailoring of structures and materials*. The royal society, 2000. 358: p. 211-227.
10. Xie, Y.M. and G.P. Steven, *Simple evolutionary procedure for structural optimization*. *Computers and Structures*, 1993. 49(5): p. 885-896.
11. Mantyla, M., *An introduction to solid modeling*, ed. C.S. Press. 1988.
12. Stroud, I., *Boundary Representation Modelling Techniques*, ed. Springer-Verlag. 2006, London.
13. Cuilliere, J.-C., *An adaptive method for the automatic triangulation of 3D parametric surfaces*. *Computer Aided Design*, 1998. 30: p. 139-149.
14. Foucault, G., et al., *An extension of the advancing front method to composite geometry*, in *Proceedings of the 16 th International Meshing Roundtable*. 2007.
15. Francois, V. and J.-C. Cuilliere, *An a priori adaptive 3D advancing front mesh generator integrated to solid modeling*. *Recent Advances in Integrated Design and Manufacturing in Mechanical Engineering*, 2003: p. 337-346.
16. Sheffer, A., et al., *Virtual topology operators for meshing*. *International Journal of Computational Geometry and Applications*, 2000. 10(3): p. 309-331.
17. Geuzaine, C. and J.-F. Remacle, *Gmsh: a three-dimensional finite element mesh generator with built-in pre- and post-processing facilities*. *International Journal for Numerical Methods in Engineering*, 2009. 79(11): p. 1309-1331.
18. Chen, C.-Y. and K.-Y. Cheng, *A direction-oriented sharpness dependent filter for 3D polygon meshes*. *Computers & Graphics*, 2008. 32(2): p. 129-140.